# A New Algorithm for Processing Interferometric Data-Stacks: SqueeSAR

Alessandro Ferretti, *Member, IEEE*, Alfio Fumagalli, Fabrizio Novali, Claudio Prati, Fabio Rocca, and Alessio Rucci

***Abstract*—Permanent Scatterer SAR Interferometry (PSInSAR) aims to identify coherent radar targets exhibiting high phase stability over the entire observation time period. These targets often correspond to point-wise, man-made objects widely available over a city, but less present in non-urban areas. To overcome the limits of PSInSAR, analysis of interferometric data-stacks should aim at extracting geophysical parameters not only from point-wise deterministic objects (i.e., PS), but also from distributed scatterers (DS). Rather than developing hybrid processing chains where two or more algorithms are applied to the same data-stack, and results are then combined, in this paper we introduce a new approach, SqueeSAR, to jointly process PS and DS, taking into account their different statistical behavior. As it will be shown, PS and DS can be jointly processed without the need for significant changes to the traditional PSInSAR processing chain and without the need to unwrap hundreds of interferograms, provided that the coherence matrix associated with each DS is properly "squeezed" to provide a vector of optimum (wrapped) phase values. Results on real SAR data, acquired over an Alpine area, challenging for any InSAR analysis, confirm the effectiveness of this new approach.**

***Index Terms*—Coherence matrix, distributed scatterers (DS), InSAR, permanent scatterers, space-adaptive filtering.**

## I. Introduction

SINCE its introduction in the late 1990s, the Permanent Scatterer (PS) technique [1]–[4] for the processing of multi-temporal radar acquisitions has gained increasing attention within the scientific community involved in the development of interferometric synthetic aperture radar (InSAR) algorithms. Indeed, PSInSAR[1] was the first of a family of technologies now referred to as Persistent Scatterer Interferometry (PSI) [5]–[10].

PSInSAR aims to identify coherent radar targets exhibiting high phase stability over the whole time period of observation. These targets, only slightly affected by temporal and geometrical decorrelation, often correspond to point-wise scatterers and are typically characterized by high reflectivity values generated by dihedral reflection or simple (deterministic) single-bounce scattering [11]. Man-made structures, boulders, and outcrops can all generate good PS.

Displacement time-series can be retrieved also for natural targets where no dominant scatterer can be identified within a certain resolution cell, but typically the estimated time-series of deformation is noisier compared to the signal retrieved for a point-wise bright scatterer and the spatial density of these measurement points is typically very low ($<$ 10 PS/sqkm, depending on the coherence threshold used to define a PS), compared to the PS density in urban areas ($>$ 100 PS/sqkm for multi-temporal C-band satellite data).

A more thorough analysis shows that, rather than corresponding to point-wise PS, these measurement points often correspond to image pixels belonging to areas of *moderate* coherence in *some* interferometric pairs of the available dataset, where many neighboring pixels share similar reflectivity values, as they belong to the same object. These targets, referred to as distributed scatterers (DS), usually correspond to debris areas, non-cultivated land with short vegetation or desert areas. Although the average temporal coherence of these natural radar targets is typically low, due to both temporal and geometrical decorrelation phenomena [12], the number of pixels sharing the same statistical behavior can be high enough to make it possible for a few of them to exceed the coherence threshold and become PS.

The need for a data fusion algorithm to properly combine PS and DS to increase the density of measurement points has been already highlighted by many authors [13]–[15]. Theoretically, one would like to increase the spatial density of measurement points over areas characterized by DS, while preserving the high-quality information obtained using the PS technique over deterministic targets. More precisely, one would like to spatially average the data over statistically homogeneous areas, increasing the signal-to-noise ratio (SNR), without compromising the identification of coherent point-wise scatterers and possibly without the need to carry out time-consuming phase unwrapping procedures on hundreds of interferograms (as requested in the conventional SBAS approach [13], [16]).

Rather than developing hybrid processing chains where two or more algorithms are applied to the same data-stack, and results are then combined, in this paper we introduce a new approach, SqueeSAR[2] [17], [18], to jointly process PS and DS,

Manuscript received November 12, 2010; revised January 14, 2011; accepted February 20, 2011. Date of publication May 12, 2011; date of current version August 26, 2011.

A. Ferretti is with Tele-Rilevamento Europa (T.R.E.), 20149 Milano, Italy (e-mail: alessandro.ferretti@treuropa.com).

A. Fumagalli, F. Novali, and A. Rucci are with the R&D, Tele-Rilevamento Europa (T.R.E.), 20149 Milan, Italy (e-mail: alfio.fumagalli@treuropa.com; fabrizio.novali@treuropa.com; alessio.rucci@treuropa.com).

C. Prati was with the Politecnico, Elettronica ed Informazione, Milan, Italy. He is now with DEI Polimi, 20133 Milano, Italy (e-mail: prati@elet.polimi.it).

F. Rocca is with the Elettronica ed Informazione, Politecnico, 20133 Milano, Italy (e-mail: rocca@elet.polimi.it).

Digital Object Identifier 10.1109/TGRS.2011.2124465

[1]Trademark registered by Politecnico di Milano (POLIMI). Patent granted to POLIMI.

[2]Trademark registered by TRE. Patent pending.

taking into account their different statistical behavior. As it will be shown, PS and DS can be jointly processed without the need for significant changes in the traditional PSInSAR processing chain.

The paper is organized as follows: Section II provides a statistical characterization of DS and an algorithm which allows them to be jointly processed with PS. Section III introduces and explains in detail the SqueeSAR algorithm. Real data results are provided, along with a comparison with PSInSAR results in Section IV, while conclusions and future research efforts are drawn in Section V.

## II. Distributed Scatterers

To overcome the limits of PSInSAR and increase the density of measurement points and the quality of the time-series over non-urban areas, the analysis of interferometric data-stacks should aim at extracting geophysical parameters not only on point-wise deterministic objects (i.e., PS), but also on distributed scatterers (DS), whose statistical description can vary significantly as a function of the parameters of the sensor used for the acquisitions and the kind of objects illuminated by the radar signal.

The exploitation of "temporary PS" or "semi-PS," i.e., deterministic scatterers behaving as PS only on a sub-set of images of the data-stack [19], although useful and effective in some cases, does not significantly change of the performance of the PSInSAR approach over non-urban areas.

Unlike PS, DS corresponding to natural targets are affected by temporal, geometrical and volumetric decorrelation [12], [14], [20] leading to lower SNR values for the interferometric phase. Consequently, the estimates of the parameters of interest are also noisier (e.g., average target velocity, elevation, displacement time-series), at least as long as data are processed independently pixel-by-pixel, as with conventional PS analyzes.

If we compare the results of PSInSAR analysis with the differential interferograms generated using an available data-set, it is often clear that the PSInSAR approach struggles to extract all available information for areas characterized by DS, where, however, simple moving average filters can strongly improve the SNR of the interferometric fringes at the cost of a decrease in resolution—a well known fact by those who typically apply interferogram stacking techniques [21], [22] or SBAS [16], [23].

Therefore, under the assumption that radar returns and the geophysical parameters of interest (e.g., the displacement vector) are common to all pixels belonging to a certain area, it should be desirable to process them jointly to enhance the SNR and improve the quality of any parameter estimation procedure. Since information associated with point-wise PS should be preserved in any filtering procedure (coherent PS should not be averaged with possible low-SNR neighboring pixels), the spatial filter to be implemented should be *space adaptive*, i.e., able to average statistically homogeneous pixels (SHP) only, without compromising the point-wise information associated to point targets.

### A. Space Adaptive Filtering: The DespecKS Algorithm

Space adaptive processing or variable support filtering is well known within the SAR community working on amplitude SAR data. Indeed, most speckle filtering techniques aimed at improving radiometric data quality while preserving image details are based on a space adaptive filter [24]. Space adaptive filters have also been applied to interferogram filtering [25], as well as to the estimation of complex coherence values. The latest can be severely biased whenever the estimation window is comprised of pixels belonging to different radar targets, characterized by different radar signatures [26]. Statistically homogeneous areas also have to be identified to accurately estimate covariance or coherency matrixes in PolSAR and PolInSAR data [27], [28] and effectively apply target decomposition theorems [28]. In general, without a proper estimation of local statistics, geophysical parameters associated to radar targets cannot be estimated effectively.

The key element of the space adaptive filtering procedure presented here is the definition of a statistical test capable of discriminating whether two image pixels belonging to an interferometric data-stack can be considered *statistically homogeneous* or not. Once the proper estimation window has been defined for each image pixel, by carefully selecting SHP families, amplitude data can be despeckled, interferometric phase values can be filtered and coherence values can be estimated properly.

It should be noted that, despite the fact that this paper is focused on the analysis of multi-temporal InSAR data-sets, the algorithm described in this section can be applied to general multi-dimensional SAR systems.

Given a set of $N$ SAR images, supposed properly re-sampled on the same master-grid, let $\mathbf{d}$ be the complex data vector

$$\mathbf{d}(P) = [d_1(P), d_2(P), \ldots, d_N(P)]^T$$

where $^{\mathrm{T}}$ indicates transposition, $P$ is a generic image pixel, $d_i(P)$ is the complex reflectivity value of the $i$th image of the data-stack corresponding to pixel $P$.

For point scatterers, $\mathbf{d}$ is an $N$-dimensional *deterministic* vector, while for distributed radar targets, where no dominant scatterer can be identified within a resolution cell, $\mathbf{d}$ is a (complex) *random* vector.

Given two data vectors $\mathbf{d}(P_1)$ and $\mathbf{d}(P_2)$ the two image pixels $P_1$ and $P_2$ will be defined as statistically homogenous if the null hypothesis that the two vectors are drawn from the same probability distribution function (p.d.f.) cannot be disproved, to a certain required level of significance. Practically, for each image-pixel, statistical tests are applied to all pixels within a certain estimation window centered on the pixel under analysis, to carefully select a homogeneous statistical population.

A possible option for this purpose is the well-known two-sample Kolmogorov-Smirnov (KS) test [29]–[31]: easy to implement, non parametric, not designed for a specific class of probability distribution functions and applicable with high reliability to data-stacks with as little as 8 images [29]. Since the KS test can be applied to real data vectors rather than complex reflectivity values, and following the conventional PS approach where the statistics of amplitude data is used as a proxy for phase stability [4], the test is applied to vectors of

amplitude values of radar reflectivity, rather than to real and/or imaginary parts.

More precisely, given a SAR data-stack of $N$ images, the sorted list of amplitude values ($\mathbf{x} = |\mathbf{d}|$) of a certain image-pixel can be easily converted to an unbiased estimator $S_N(x)$ of the cumulative distribution function (c.d.f.) of the p.d.f. from which it is drawn that

$$S_N(X) = \begin{cases} 0, & \text{if } X < x_1 \\ \frac{k}{N}, & \text{if } x_{\mathrm{k}} \leq X < x_{\mathrm{k+1}} \\ 1, & \text{if } X \geq x_N \end{cases} \quad (1)$$

where $x_{\mathrm{i}}$ is the ith element of the list of amplitude values.

To evaluate whether two image-pixels $P_1$ and $P_2$ are SHP (i.e., have amplitude data drawn from the same p.d.f.), the two-sample KS test measures the maximum value ($D_{\mathrm{N}}$) of the absolute difference between their cumulative distribution functions, $S_N^{P1}$ and $S_N^{P2}$

$$D_N = \sqrt{N/2}\sup_{\mathrm{x}\in\mathrm{R}} \left| S_N^{P1}(x) - S_N^{P2}(x) \right|. \quad (2)$$

The distribution of $D_N$ can be approximated by the KS distribution, whose c.d.f. $H(t)$ is given by [29]–[31]

$$\begin{aligned} P(D_N \leq t) &= H(t) \\ &= 1 - 2\sum_{n=1}^{\infty} (-1)^{\mathrm{n}-1} e^{-2\mathrm{n}^2\mathrm{t}^2} \end{aligned} \quad (3)$$

and does not depend on the specific c.d.f. of the data. The KS test considers the two data vectors drawn from the same statistical population if $D_N \leq c$, where the threshold $c$ depends on the fixed significance level $\alpha$ and can be found from the condition

$$\alpha = 1 - H(t) \quad (4)$$

It should be noted that, since the KS test is invariant under reparametrization of the random variates under analysis, the same significance of the test would be obtained working on either a linear or logarithmic scale applied to amplitude data and using amplitude or intensity values.

The space–variant algorithm developed for the identification of statistically homogeneous areas, DespecKS,[3] can be presented schematically as follows:

1) For each image-pixel $P$, define an estimation window centered on $P$ where pixels sharing the same statistics as $P$ have to be identified.
2) By applying the two-sample KS test to amplitude data vectors, all pixels within the estimation window that can be considered as statistically homogeneous with $P$ are selected, given a certain level of significance.
3) Discard image-pixels that, though selected by the KS test, are not connected to $P$ directly or through other SHP.
4) Pixel $P$ and all SHP within the estimation window connected to $P$ are then considered as a homogeneous statistical population (identified in the following as set $\Omega$) for further processing and analysis.

[3]Trademark registered by TRE. Patent pending.

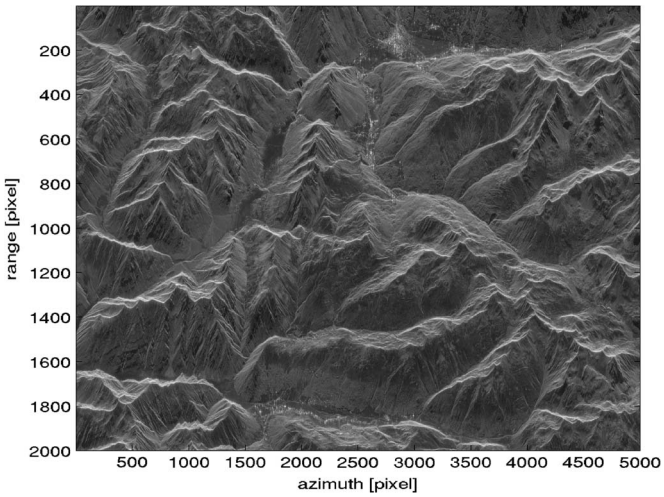


Fig. 1. Multi-image reflectivity map (incoherent average of 65 RADARSAT scenes) of the Alpine region used as a test site. The extent of the area is about $20 \times 25$ km.

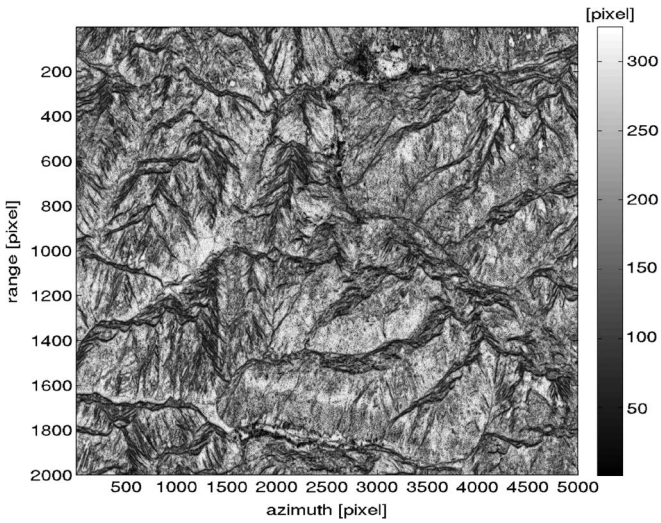


Fig. 2. Number of SHP identified by the KS test.

Step 3 reduces the number of SHP identified by the KS test but is included to increase the probability that nearby pixels belong to the same radar target and share the same geophysical parameters.

The defined space adaptive filter can be used as: (1) a *despeckle filter* to be applied either to each SAR image or to the average reflectivity map of the area, by simply averaging amplitude or intensity values of SHP. The result is a reduction of speckle noise over homogeneous areas (such as agricultural fields, forests, etc.) without affecting point-wise targets (such as buildings, boulders, and outcrops); and (2) an estimator of the complex coherence of any interferogram generated from the available SAR data-set, whenever the number of SHP surrounding the pixel under analysis is high enough (see next section).

In Fig. 2 we show the number of SHP identified by the KS test for the alpine region represented in Fig. 1 (see Section IV). The dimensions of the window used to identify SHP is about a hectare, which corresponds in pixels to a window of $15 \times 21$. Visual comparison between Figs. 1 and 2 shows how the

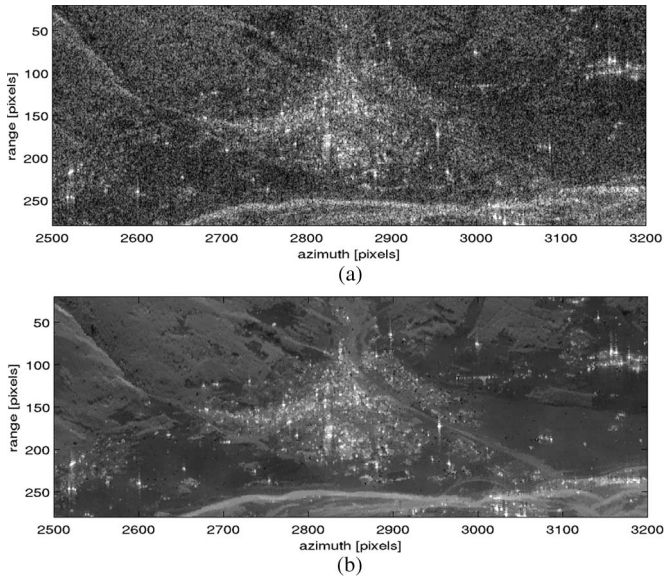


Fig. 3. Comparison between: (a) a close-up of a reflectivity image (single SAR scene, amplitude data), and (b) its filtered version obtained by applying the DespecKS algorithm.

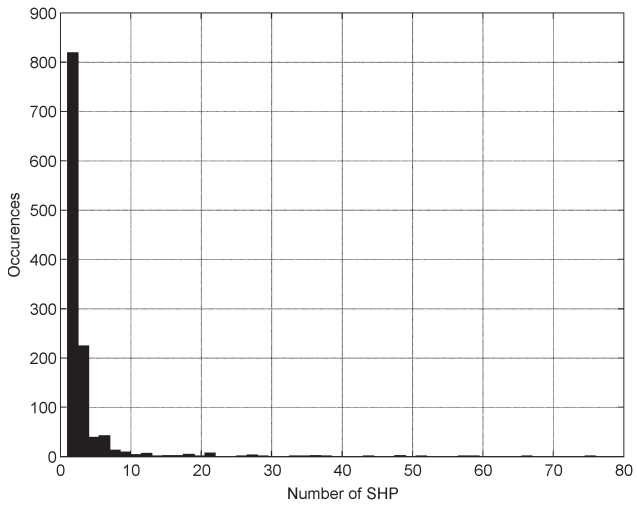


Fig. 4. Histogram of the number of SHP for targets exhibiting a temporal coherence higher than 0.8.

KS test indentifies a high number of SHP over homogenous areas, while in urban areas and ridges, the number of SHP is very low.

The efficiency of the despeckle filtering is proven by a comparison between Fig. 3(a) and (b), in fact we notice a significant reduction in speckle noise over non-urban areas without blurring the point scatterers present in the image, as can be seen in Fig. 3(b). Where, for example, the sidelobes of strong scatterers are preserved.

Analysis of the distribution of SHP applied to the PS population shows that most of the PS correspond to isolated pixels. More precisely, results on real data (Section IV) have shown that 95% of PS exhibiting a temporal coherence greater than 0.8 have less than 20 SHP (see Fig. 4), corresponding to about 8 independent looks, in SAR data interpolated by a factor of 2 in range direction only. Therefore, by fixing 20 as the minimum number of SHP on which a spatial filtering can be carried out, it is possible to preserve PS information.

It should be noted that the KS test is just one (and probably the easiest) option to design the algorithm for SHP identification, based on a data-stack of SAR scenes. Although simple and effective, the KS test is almost insensitive to different extremal values of the two data vectors under test. For instance, a very high radar return (i.e., a spike) affecting just one of the two data vectors will not be enough to differentiate the two pixels under analysis, that will be considered SHP. Indeed, a limit of the KS test is its poor sensitivity to deviations from the hypothesized distribution that occur in the tails. To overcome this limit, several modified KS tests have been proposed [31]. The basic idea is to introduce a weighting function into the test to make it consistent with respect to local deviations that may occur in the tails or in the middle of the distribution [32], [33]. The drawback with this formulation is in determining the reasonable criteria for the choice of optimum weighting functions. Although the Anderson–Darling test [31], [34] can represent another interesting option to consider.

### *B. Statistical Description of Distributed Scatterers*

The DespecKS algorithm, described in the previous paragraph, is an important tool to properly estimate the statistical parameters of each DS. In fact, under the Gaussian scattering assumption based on the central limit theorem [35], SAR data vector can be described by a zero-mean, multi-dimensional, complex Gaussian p.d.f. Thus, for a complete statistical characterization of a DS it is sufficient to know the covariance (or correlation) matrix.

After identification of the SHP of pixel $P$, it is possible to estimate the sample covariance matrix given by

$$\mathbf{C}(P) = E[\mathbf{d}\mathbf{d}^{\mathrm{H}}] \approx \frac{1}{|\Omega|}\sum_{P\in\Omega}\mathbf{d}(P)\mathbf{d}(P)^{\mathrm{H}} = \widehat{\mathbf{C}} \qquad (5)$$

where $^{\mathrm{H}}$ indicates Hermitian conjugation and $\Omega$ is the set of SHP used in the sample estimate of the covariance matrix.

It is worth noting how the principal diagonal of the covariance matrix of any DS is actually a data vector of $N$ despeckled (because spatially averaged) intensity values of the $N$ available scenes, while the phase values of the off-diagonal complex elements of $\hat{\mathbf{C}}$ correspond to spatially filtered interferograms.

A thorough analysis of the properties of covariance matrixes associated to single-polarization multi-temporal SAR data-sets is beyond the scope of this paper [40]. Suffice it to say, however, that since the covariance matrix and its eigen-decomposition have been exploited successfully in a PolSAR and PolInSAR context for classification purposes [28], most of the algorithms developed for polarimetric data could be applied to $\hat{\mathbf{C}}$.

Whenever amplitude data are normalized such that $E[|d_i|^2] = 1$, for all $i$, a coherence matrix $\mathbf{\Gamma}$ is obtained. Working on coherence matrixes rather than covariance matrixes can be beneficial to compensate for possible backscattered power unbalances among all the images (similarly to the computation of the temporal coherence in PSInSAR, where all amplitude values are normalized). Absolute values of the

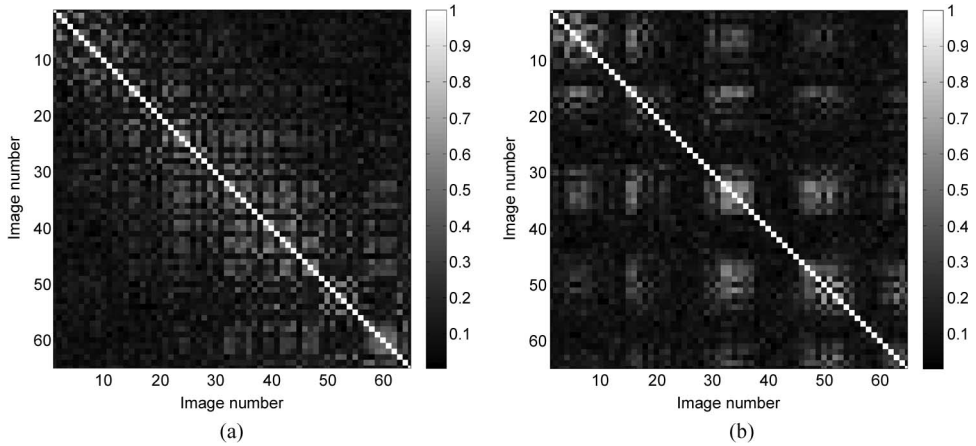


Fig. 5. Two examples of absolute values of coherence matrices estimated from the data, showing how the decorrelation mechanisms can significantly differ among DS. The shape of the first example of $\mathbf{C}$ is typical for those DS which are mainly affected by temporal decorrelation. The second kind presents a seasonal behavior revealing a loss in coherence due to snowfall in the winter period.

off-diagonal elements of $\hat{\mathbf{\Gamma}}$ are actually an estimate of the coherence values [36] for all possible interferograms of the data-stack $(\gamma_{\mathrm{kj}})$, In Fig. 5 we show two examples of $\mathbf{C}$ exhibiting different decorrelation mechanisms, while the loss in coherence of $\mathbf{C}$ in Fig. 5(a) is mostly due to temporal decorrelation. In Fig. 5(b), we mainly notice a seasonal behavior in $\mathbf{C}$, related to snowfall in the winter period.

The phase values of the coherence matrix, as for the sampled covariance matrix, correspond instead to spatially filtered interferometric phases $(\phi_{\mathrm{kj}})$

$$\widehat{\mathbf{\Gamma}} = \{\gamma_{\mathrm{kj}} \cdot e^{\mathrm{i}\phi_{\mathrm{kj}}}\} \tag{6}$$

The correlation matrix is a Hermitian matrix and its eigendecomposition is just a sum of outer products of its eigenvectors $(\mathbf{u}_{\mathrm{n}})$, weighted by their eigenvalues $(\sigma_{\mathrm{n}})$

$$\mathbf{\Gamma} = \sum_{\mathrm{n}=1}^{N} \sigma_{\mathrm{n}} \mathbf{u}_{\mathrm{n}} \mathbf{u}_{\mathrm{n}}^{\mathrm{H}} \tag{7}$$

The coherence matrix associated with an ideal PS is equal, instead, to a singular matrix having just one non-zero eigenvalue and eigenvector and all moduli equal to 1

$$\mathbf{\Gamma}(PS) = \mathbf{1}e^{\mathrm{i}\boldsymbol{\theta}} \cdot (\mathbf{1}e^{\mathrm{i}\boldsymbol{\theta}})^{\mathrm{H}} \tag{8}$$

where $\boldsymbol{\theta} = [\theta_1, \theta_2, \ldots, \theta_N]^T$ is simply the vector of the phase values of the $N$ available images in correspondence to the PS. Therefore, for an ideal PS, no matter which image pairs are used to generate the interferogram, the coherence is always 1.

### C. Phase Triangulation Algorithm

For a deterministic radar target, such as a PS, the phase values of all off-diagonal elements of the coherence matrix are redundant: the $N(N-1)/2$ phase values (the matrix is Hermitian) are simply the difference in phase values of the $N$ available SAR scenes, so the following equation holds:

$$\begin{aligned} \angle\left(\{\widehat{\mathbf{\Gamma}}\}_{\mathrm{nj}}\right) &= \angle\left(\{\widehat{\mathbf{\Gamma}}\}_{\mathrm{nm}} \cdot \{\widehat{\mathbf{\Gamma}}\}_{\mathrm{jm}}^{*}\right) \\ &= \theta_{\mathrm{n}} - \theta_{\mathrm{j}} \qquad n, m, j = 1, \ldots, N \end{aligned} \tag{9}$$

where the operator $\{\cdot\}_{\mathrm{jm}}$ indicates the element of the matrix at raw $j$ and column $m$. In other words, in case of deterministic radar targets, the property of phase triangularity, or phase consistency, is met by the construction

$$\phi_{nj} = \phi_{nm} - \phi_{mj} \tag{10}$$

This is no longer true for a DS. The coherence matrix is not redundant (it is not rank 1) and, in general, (10) does not hold. Indeed, the *filtered* interferogram generated by image $n$ and image $j$ is not equal to the phase difference between the *filtered* interferograms generated using the image pair $(n, m)$ and $(m, j)$. Then, for a DS, we are somewhat forced to deal with $N(N-1)/2$ interferometric phase values and not simply $N$, as with PS.

Incidentally, this is reason why in the SBAS algorithm, even after successfully phase unwrapping a sub-set of possibly high-coherence interferograms connecting all images within a data set, the Singular Value Decomposition (SVD) is applied to the data as a tool to retrieve the time-series of deformation: spatially filtered phase values are not consistent and 3-D phase unwrapping algorithms cannot be applied to filtered data.

A key problem is then related to the estimation of a vector of $N$ phase values, $\boldsymbol{\vartheta} = [\vartheta_1, \vartheta_2, \ldots, \vartheta_N]$, matching those of the off-diagonal elements of $\hat{\mathbf{\Gamma}}$, properly taking into account the associated coherence values (i.e., the moduli of $\hat{\mathbf{\Gamma}}$).

To create the right framework for this optimization, we suppose that the coherence matrix of a generic pixel $P$ can be expressed as follows:

$$\mathbf{\Gamma}(P) = \mathbf{\Theta}\mathbf{\Upsilon}\mathbf{\Theta}^{\mathrm{H}} \tag{11}$$

where:

- $\boldsymbol{\Upsilon}$ is an $N \times N$ symmetric *real*-value matrix whose elements correspond to the coherence values of all the interferograms.
- $\boldsymbol{\Theta}$ is an $N \times N$ diagonal matrix, $\boldsymbol{\Theta} = \mathrm{diag}\{\exp(j\boldsymbol{\theta})\}$, containing the values of the "true" phase values of pixel $P$, related to the optical path of the radar beam in each acquisition.

Under the assumption that all pixels belonging to $\Omega$ are described by the same set of phase values $\theta$, the p.d.f. of the SHP can then be expressed as [37]

$$p(\mathbf{d}_\Omega|\boldsymbol{\theta}) \propto \prod_{\mathrm{P}\in\Omega} \exp\left(-\mathbf{d}_\mathrm{P}^\mathrm{H}\boldsymbol{\Theta}\boldsymbol{\Upsilon}^{-1}\boldsymbol{\Theta}^\mathrm{H}\mathbf{d}_\mathrm{P}\right) = \exp\left[-\mathrm{trace}(\boldsymbol{\Theta}\boldsymbol{\Upsilon}^{-\mathbf{1}}\boldsymbol{\Theta}^\mathrm{H}\hat{\boldsymbol{\Gamma}})\right] \tag{12}$$

and so the maximum likelihood (ML) estimate of $\theta$ is obtained by maximizing this p.d.f. or minimizing the absolute value of its logarithm.

Since only phase differences appear in $\hat{\boldsymbol{\Gamma}}$, phase values can be estimated up to an arbitrary additive constant. Without loss of generality, we can set the interferometric phase of the first image to zero.

The optimal estimate of the $N-1$ phase values, $\boldsymbol{\lambda} = [0, \vartheta_2, \ldots, \vartheta_N]^T$, is then given by

$$\begin{aligned}\hat{\boldsymbol{\lambda}} &= \arg\max_{\lambda}\left\{\exp\left[-\mathrm{trace}(\boldsymbol{\Phi}\boldsymbol{\Upsilon}^{-\mathbf{1}}\boldsymbol{\Phi}^\mathrm{H}\hat{\boldsymbol{\Gamma}})\right]\right\} \\ &= \arg\max_{\lambda}\left\{\exp\left[-\boldsymbol{\Lambda}^\mathrm{H}(\boldsymbol{\Upsilon}^{-\mathbf{1}}\circ\hat{\boldsymbol{\Gamma}})\boldsymbol{\Lambda}\right]\right\} \\ &= \arg\max_{\lambda}\left\{\boldsymbol{\Lambda}^\mathrm{H}(\boldsymbol{\Upsilon}^{-\mathbf{1}}\circ\hat{\boldsymbol{\Gamma}})\boldsymbol{\Lambda}\right\}\end{aligned} \tag{13}$$

where:

- $\boldsymbol{\Phi}$ is an $N \times N$ diagonal matrix, $\boldsymbol{\Phi} = \mathrm{diag}\{\exp(i\boldsymbol{\lambda})\}$
- $\boldsymbol{\Lambda}$ is an $N$-dimensional vector, $\boldsymbol{\Lambda} = \exp(i\boldsymbol{\lambda})$
- $\circ$ represents the Hadamard (i.e., entry-wise) product.

Since the "true" coherence matrix $\boldsymbol{\Upsilon}$ is unknown, one can use an estimate of $\boldsymbol{\Upsilon}$ as the absolute value of $\hat{\boldsymbol{\Gamma}}$

$$\hat{\boldsymbol{\lambda}} = \arg\max_{\lambda}\left\{\boldsymbol{\Lambda}^\mathrm{H}\left(|\hat{\boldsymbol{\Gamma}}|^{-\mathbf{1}}\circ\hat{\boldsymbol{\Gamma}}\right)\boldsymbol{\Lambda}\right\} \tag{14}$$

The drawbacks of this solution are due to the fact that coherence estimates are biased [26] and the matrix $|\hat{\boldsymbol{\Gamma}}|$ is not, in general, positive and definite as with $\hat{\boldsymbol{\Gamma}}$. For this reason, before matrix inversion, it is usually necessary to insert a damping factor to avoid small negative or null eigenvalues.

The algorithm requires the minimization of a nonlinear functional, implying the use of iterative methods. A possible solution is the BFGS (Broyden–Fletcher–Goldfarb–Shanno) algorithm, which is a quasi-Newton method for unconstrained nonlinear optimization [29]. Another option to deal with bad-conditioned matrixes is to rely on the eigen-decomposition of $|\hat{\boldsymbol{\Gamma}}|$ and use its generalized inverse or pseudoinverse.

Once the optimal solution has been obtained, the quality of the estimated phase values $\theta_\mathrm{i}$ should be assessed. A possible "goodness of fit" measure is the following:

$$\gamma_\mathrm{PTA} = \frac{1}{N^2-N}\sum_{n=1}^{N}\sum_{k\neq n}^{N} e^{i\phi_{nk}}e^{-i(\vartheta_n-\vartheta_k)} \tag{15}$$

which can be also written as

$$\gamma_\mathrm{PTA} = \frac{2}{N^2-N}\mathrm{Re}\sum_{n=1}^{N}\sum_{k=n+1}^{N} e^{i\phi_{nk}}e^{-i(\vartheta_n-\vartheta_k)}. \tag{16}$$

Indeed, $\gamma_\mathrm{PTA}$ can be seen as an extension, for DS, to the temporal coherence [1], [2], [38] widely used in PS analyzes.

It should be noted that, by applying the phase triangulation algorithm (PTA) described above, the phase values of each DS are actually filtered *before* any phase unwrapping, taking into account *all* possible interferograms. Once $N$ optimum phase values are available, 3-D phase unwrapping algorithm [39] can then be performed.

## III. SqueeSAR

In the previous sections, the two main concepts applied in the new SqueeSAR approach have been presented. The first one is the DespecKS algorithm, for the identification of SHP families used in the estimation of the sampled coherence matrix and the statistical characterization of each DS, preserving the information of point-wise PS. The second one is the PTA, which provides the bridge between PS and DS and making it possible to characterize a DS through $N$ phase values (as for PS), rather than $N(N-1)/2$, at least for DS exhibiting high enough $\gamma_\mathrm{PTA}$ values.

By applying these tools, it is possible to pre-process the available data set so that both PS and DS can be exploited successfully, using the standard PSInSAR processing chain.

The SqueeSAR algorithm can be described as follows:

1) Apply the DespecKS algorithm to identify, for each pixel $P$, the family of SHP. Let $N_\mathrm{S}$ be the number of SHP.
2) Define DS all those pixels for which $N_\mathrm{S}$ is larger than a certain threshold.
3) For all DS, estimate the sample coherence matrix taking advantage of the SHP families identified in Step 1 above.
4) Apply the PTA algorithm to each coherence matrix associated to each DS.
5) Select the DS exhibiting a $\gamma_\mathrm{PTA}$ value higher than a certain threshold and substitute the phase value of the original SAR images with their optimized values.
6) Process the selected DS jointly with the PS using the traditional PSInSAR algorithm for the estimation of the displacement time-series of each measurement point.

As already mentioned, it is worth pointing out that, using the SqueeSAR approach, the $N$ phase values that best fit the phases of the sample coherence matrix are retrieved before any phase unwrapping algorithm: this represents one of the most relevant differences compared to many other algorithms, such as SBAS [23]. It is well known phase unwrapping is the most delicate and difficult phase of any InSAR processing chain, as hundreds of interferograms should be successfully unwrapped to effectively estimate the deformation field. In SqueeSAR, the

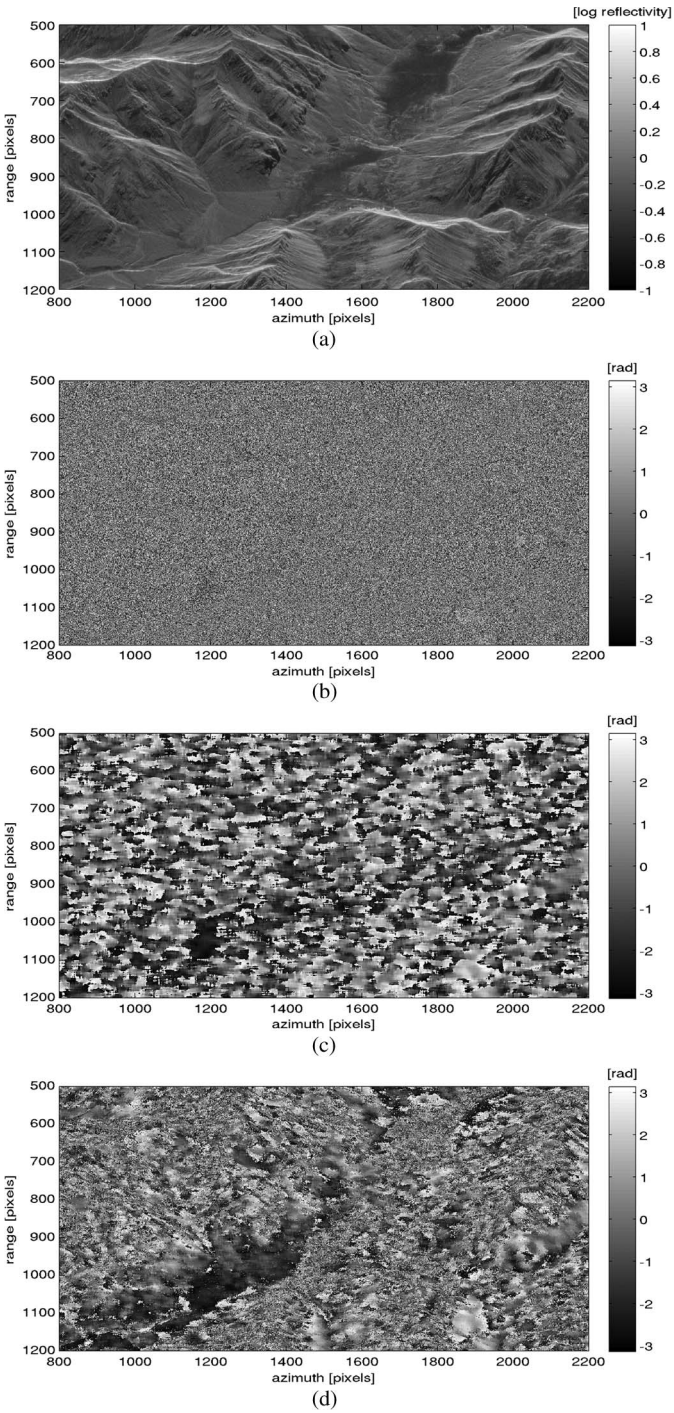


Fig. 6. (a) Reflectivity map of the region considered to compare (b) a full resolution interferometric phase, (c) the multi-looked interferogram filtered using a $13 \times 25$ boxcar kernel and (d) the interferogram reconstructed applying the PTA algorithm. The normal baseline of the interferogram under analysis is 600 m and the temporal baseline 200 days.

optimum $N$ phase values are properly combined *before* any phase unwrapping occurs. This is an important procedure as the interferometric phases "reconstructed" by applying the PTA are less noisier than the spatially filtered interferometric phases, making more robust the spatial phase unwrapping procedure (see Section IV, Fig. 6).

Another significant difference with respect to other multi-interferogram algorithms is the use of *all* possible interferograms to estimate the optimum phase values, not only a subset of them, selected based on a *model* for target coherence. In fact, any interferogram can provide useful information, according to its coherence level. Since SqueeSAR is based on the analysis of the correlation matrix, all possible interferograms are generated and the associated coherence values are computed, no matter the temporal or geometrical baseline.

The last important aspect concerns the implemented spatial filtering technique. By means of the DespecKS algorithm, only SHP-families are averaged, preserving the information associated to point-wise radar targets, which are identified as isolated pixels by the test and, as a consequence, are not affected by the filtering procedure.

The term SqueeSAR is related to the concept of "squeezing" the information associated to the coherence matrix to retrieve a vector of optimum phase values to be used for interferometric analysis.

## IV. Results on Real Data

To assess the improvements related to the new algorithm, we selected an Alpine region in Italy, relatively challenging for InSAR analysis due to its rough topography and vegetation. 65 descending RADARSAT images acquired from April 2003 to March 2008 were processed. All data were interpolated by a factor of two in range direction and re-sampled on the same master acquisition (November 19, 2005). In Fig. 1, the incoherent average of all the SAR scenes (multi-image reflectivity map) is reported. The area is approximately $20 \times 25$ km wide.

The data-set was processed using both the standard PSInSAR approach and the new SqueeSAR algorithm. To implement the new processing, the DespecKS algorithm was applied to identify the SHP for each pixel. Whenever the number of SHP exceeded 20 pixels ($N_{\mathrm{S}} = 20$) the coherence matrix was estimated and the PTA was applied to retrieve the $N$ optimum phase values. As one of the primary objectives of SqueeSAR is to maintain the point-wise radar responses of PS, the value of $N_{\mathrm{S}}$ is based on the results shown in Fig. 4, which shows how 95% of PS have less than 20 SHP. However, this value should not be used for all sites as it is dependent on the spatial resolution of the satellite providing the data.

After PTA, we generate $N$ differential optimally filtered interferograms. The PTA actually allow the reconstruction of any differential interferogram of interest, based on the optimum phase values estimated from the coherence matrixes. Fig. 6(a)–(c) show how effective the PTA can be. The ML estimation of the phase values can be seen as a spatial filter (since SHP are considered, not only the single pixel P) and as a temporal filter (as all InSAR pairs are properly combined).

The new differential interferograms, available after the DespecKS and the PTA steps, are used as input data for the traditional PSInSAR algorithm. By comparing Fig. 7(a) and (b), it is clearly visible how the SqueeSAR approach significantly increases the spatial density of measurement points (MP), passing from 85 PS/km$^2$ to 450 MP/km$^2$. It is now possible to better define the footprints of sliding areas and even identify new ones, not previously detected by PSInSAR (see Fig. 8).

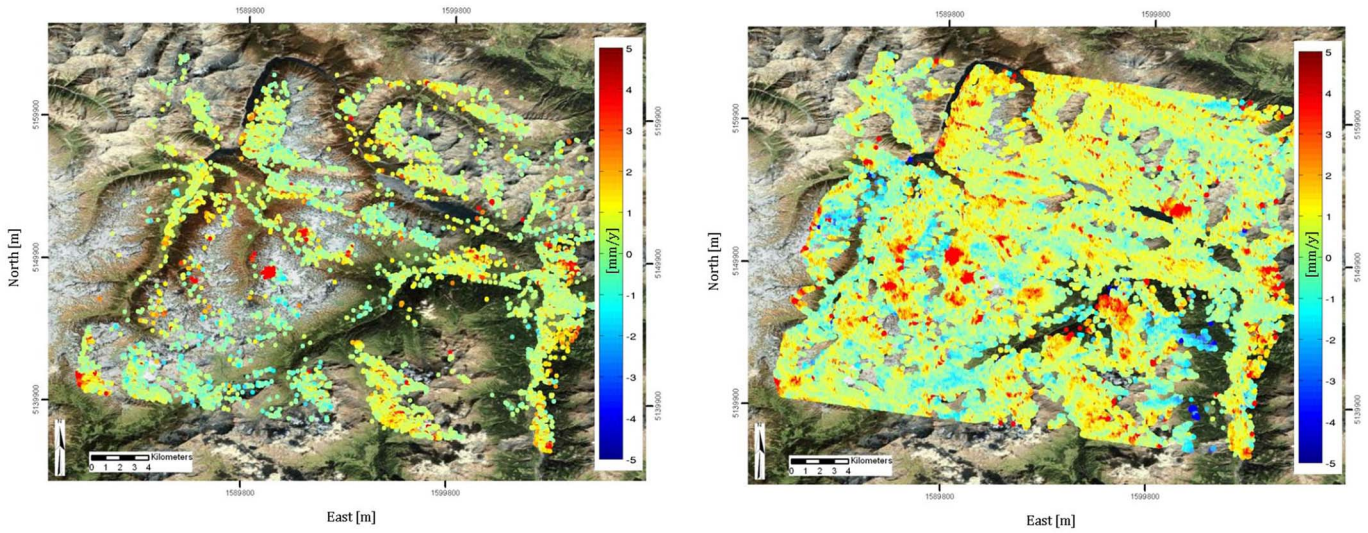


Fig. 7. Comparison between the LOS velocity map [mm/yr] estimated applying the (a) PSInSAR and the (b) SqueeSAR algorithm. A positive velocity means a movement of the target toward the satellite.

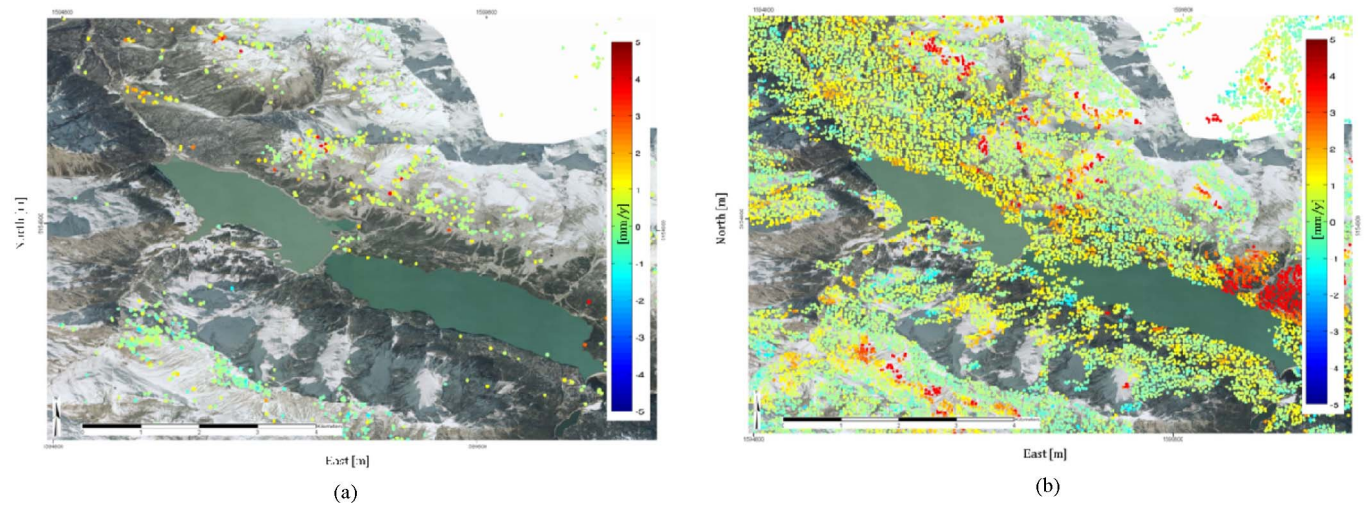


Fig. 8. LOS velocity measurements [mm/yr], obtained by (a) PSInSAR and (b) SqueeSAR, for the Cancano lakes region.

Another advantage of the new approach concerns the quality of the displacement time-series of the DS. In some cases, some DS are identified as PS by the PSInSAR processing chain, making it possible to compare the time-series of deformation estimated by SqueeSAR and that available with PSInSAR. By applying SqueeSAR, it is possible to significantly enhance the SNR resulting in a less noisy time-series, as shown in Fig. 9. For the area under analysis, mainly a mountainous region, about 6000 targets are identified as PS by the standard algorithm. Of these 6000 targets, 4000 are identified as DS by SqueeSAR. Thanks to the new processing chain, we measured an average increase in DS coherence of about 0.1.

The improvement in quality of the time-series, above the optimum estimate of the interferometric phases provided by PTA, is also due to the fact that, by increasing the spatial density of the MP, atmospheric effects can be better estimated and removed.

From a computational point of view, the improvements obtained using the SqueeSAR approach require a processing time of about four times longer than the standard PSInSAR analysis, starting from the focused and co-registered interferograms. The additional required processing time has so far been the main drawback of the new approach.

## V. Conclusion

PSInSAR is a powerful tool for monitoring urban areas, characterized by a high density of point-wise stable targets originated by man-made structures. However, all PSI algorithms struggle to provide high-quality measurements over non-urban areas characterized by DS rather than PS. On the contrary, other approaches, like conventional DInSAR, interferogram stacking, SBAS, etc., can extract information from DS with more ease than from PS, paying in accuracy of the measurements. In this paper, we have proposed a new approach, referred to as SqueeSAR, to jointly process PS and DS, taking into account their different statistical behavior. The results provided by the new algorithm clearly show how a proper synergistic analysis of PS and DS can significantly improve the density and quality of InSAR measurement points, over non-urban areas. The key-

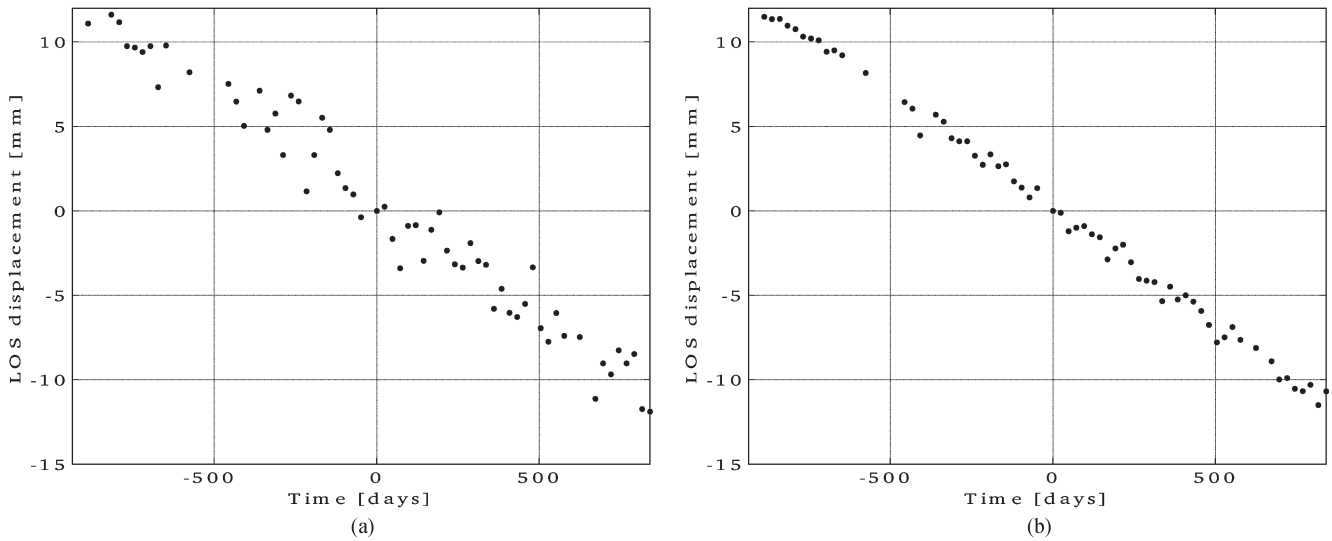


Fig. 9. Comparison between the displacement time series obtained by (a) the PSInSAR and (b) the SqueeSAR approaches for the same target.

point is the statistical characterization of the DS; the study of the covariance or coherence matrix associated with the DS will, in our opinion, be the roadmap for an advanced multi-interferogram algorithm. The name SqueeSAR resembles the very fact that the information content of these matrix should be actually "squeezed."

Noteworthy it is the introduction of two-sample statistical test for SHP identification, in a multi-image framework. Apart from allowing an effective statistical characterization of DS, the DespecKS approach proved to be a key-factor to preserve the high-quality information associated with PS.

Further work will be devoted to the optimization of the DespecKS algorithm, to deal with long-tailed distributions and reflectivity spikes, as well as the identification of robust and fast optimization algorithm for carrying out the PTA. The computational costs represent, in fact, the main drawback of the new processing chain compared to the standard PSInSAR analysis.

## ACKNOWLEDGMENT

Authors would like to thank all TRE staff for their support in data processing and S. Tebaldini, F. De Zan and A. M. Guarnieri for fruitful discussions.

## REFERENCES

[1] A. Ferretti, C. Prati, and F. Rocca, "Non-uniform motion monitoring using the permanent scatterers technique," in *Proc. 2nd Int. Workshop ERS SAR Interferometry, FRINGE*, Liège, Belgium, Nov. 10–12, 1999, pp. 1–6.

[2] A. Ferretti, C. Prati, and F. Rocca, "Nonlinear subsidence rate estimation using permanent scatterers in differential SAR interferometry," *IEEE Trans. Geosci. Remote Sens.*, vol. 38, no. 5, pp. 2202–2212, Sep. 2000.

[3] A. Ferretti, C. Prati, and F. Rocca, "Process for radar measurements of the movement of city areas and landsliding zones," International Application Published Under the Patent Cooperation Treaty (PCT), Nov. 2000.

[4] A. Ferretti, C. Prati, and F. Rocca, "Permanent scatterers in SAR interferometry," *IEEE Trans. Geosci. Remote Sens.*, vol. 39, no. 1, pp. 8–20, Jan. 2001.

[5] B. Kampes, *Radar Interferometry: Persistent Scatterer Technique*. Dordrecht, The Netherlands: Springer-Verlag, 2006.

[6] A. Hooper, H. Zebker, P. Segall, and B. Kampes, "A new method for measuring deformation on volcanoes and other natural terrains using InSAR persistent scatterers," *Geophys. Res. Lett.*, vol. 31, p. L23611, 2004. DOI: 10.1029/2004GL021737.

[7] A. Hooper, P. Segall, and H. Zebker, "Persistent scatterer interferometric synthetic aperture radar for crustal deformation analysis, with application to Volcán Alcedo, Galápagos," *J. Geophys. Res.*, vol. 112, p. B07407, 2007, DOI: 10.1029/2006JB004763.

[8] C. Werner, U. Wegmuller, A. Wiesmann, T. Strozzi, G. Sensing, and S. Muri, "Interferometric point target analysis with JERS-1 L-band SAR data," in *Proc. IGARSS*, Toulouse, France, Jul. 21–25, 2003, pp. 4359–4361.

[9] H. A. Zebker, A. P. Shanker, and A. Hooper, "InSAR remote sensing over decorrelating terrains: Persistent scattering methods," in *Proc. IEEE Radar Conf.*, 2007, pp. 717–722.

[10] D. A. Schmidt and R. Burgmann, "Time-dependent land uplift and subsidence in the Santa Clara valley, California, from a large interferometric synthetic aperture radar data set," *J. Geophys. Res.*, vol. 108, no. B9, p. 2416, 2003, DOI: 10.1029/2002JB002267.

[11] D. Perissin and A. Ferretti, "Urban target recognition by means of repeated spaceborne SAR images," *IEEE Trans. Geosci. Remote Sens.*, vol. 45, no. 12, pp. 4043–4058, Dec. 2007.

[12] H. A. Zebker and J. Villasenor, "Decorrelation in interferometric radar echoes," *IEEE Trans. Geosci. Remote Sens.*, vol. 30, no. 5, pp. 950–959, Sep. 1992.

[13] A. Hooper, "A multi-temporal InSAR method incorporating both persistent scatterer and small baseline approaches," *Geophys. Res. Lett.*, vol. 35, p. L16 302, 2008, DOI: 10.1029/2008GL03465.

[14] F. Rocca, "Modeling interferogram stacks," *IEEE Trans. Geosci. Remote Sens.*, vol. 45, no. 10, pp. 3289–3299, Oct. 2007.

[15] H. A. Zebker and A. P. Shanker, "Geodetic imaging with time series persistent scatterer InSAR," presented at the American Geophysical Union, San Francisco, CA, 2008.

[16] R. Lanari, O. Mora, M. Manunta, J. J. Mallorqui, P. Berardino, and E. Sansosti, "A small-baseline approach for investigating deformations on full-resolution differential SAR interferograms," *IEEE Trans. Geosci. Remote Sens.*, vol. 42, no. 7, pp. 1377–1386, Jul. 2004.

[17] A. Ferretti, A. Fumagalli, F. Novali, C. Prati, F. Rocca, and A. Rucci, "Exploitation of distributed scatterers in interferometric data stacks," presented at the Int. Geoscience Remote Sensing Symp. (IGARSS) Conf., Cape Town, South Africa, 2009.

[18] A. Ferretti, A. Fumagalli, F. Novali, C. Prati, F. Rocca, and A. Rucci, "The second generation PSInSAR approach: SqueeSAR," presented at the Int. Workshop ERS SAR Interferometry (FRINGE), Frascati, Italy, 2009.

[19] M. Basilico, A. Ferretti, F. Novali, C. Prati, and F. Rocca, "Advances in permanent scatterers analysis: Semi and temporary PS," in *Proc. Eur. Conf. Synthetic Aperture Radar*, Ulm, Germany, May 25–27, 2004, pp. 349–350.

[20] R. Hanssen, *Radar Interferometry: Data Interpretation and Error Analysis*. Dordrecht, The Netherlands: Kluwer, 2001.

[21] D. T. Sandwell and E. J. Price, "Phase gradient approach to stacking interferograms," *J. Geophys. Res.*, vol. 103, no. B12, pp. 30 183–30 204, Dec. 1998.

[22] S. Lyons and D. Sandwell, "Fault creep along the southern San Andreas from InSAR, permanent scatterers, and stacking," *J. Geophys. Res.*, vol. 108, no. B1, p. 2047, 2003, DOI: 10.1029/2002JB001831.

[23] P. Berardino, G. Fornaro, R. Lanari, and E. Sansosti, "A new algorithm for surface deformation monitoring based on small baseline differential SAR interferograms," *IEEE Trans. Geosci. Remote Sens.*, vol. 40, no. 11, pp. 2375–2383, Nov. 2002.
[24] R. Touzi, "A review of speckle filtering in the context of estimation theory," *IEEE Trans. Geosci. Remote Sens.*, vol. 40, no. 11, pp. 2392–2404, Nov. 2002.
[25] J. S. Lee, S. R. Cloude, K. P. Papathanassiou, M. R. Grunes, and I. H. Woodhouse, "Speckle filtering and coherence estimation of polarimetric SAR interferometry data for forest applications," *IEEE Trans. Geosci. Remote Sens.*, vol. 41, no. 10, pp. 2254–2263, Oct. 2003.
[26] R. Touzi, A. Lopes, J. Bruniquel, and P. Vachon, "Unbiased of the coherence from multi-look SAR data," *IEEE Trans. Geosci. Remote Sens.*, vol. 68, pp. 662–664, May. 1996.
[27] G. Vasile, E. Trouve, J.-S. Lee, and V. Buzuloiu, "Intensity-driven adaptive-neighborhood technique for polarimetric and interferometric SAR parameters estimation," *IEEE Trans. Geosci. Remote Sens.*, vol. 44, no. 6, pp. 1609–1621, Jun. 2006.
[28] J. Lee and E. Pottier, *Polarimetric Imaging: From Basics to Applications*. Boca Raton, FL: CRC Press, 2009.
[29] M. A. Stephens, "Use of the Kolmogorov-Smirnov, Cramér-Von Mises and related statistics without extensive tables," *J. R. Stat. Soc. Ser. B (Methodological)*, vol. 32, no. 1, pp. 115–122, 1970.
[30] W. H. Press, S. A. Teukolsky, W. T. Vetterling, and B. P. Flannery, *Numerical Recipes in C: The Art of Scientific Computing*. Cambridge, U.K.: Cambridge Univ. Press, 1988, ch. 14.
[31] P. Kwam and B. Vidakovic, *Nonparametric Statistics With Applications to Science and Engineering*. Hoboken, NJ: Wiley, 2007.
[32] D. Manson and J. Shuenemeyer, "A modified KS test sensitive to tails alternatives," *Ann. Statist.*, vol. 11, no. 3, pp. 933–946, Sep. 1983.
[33] P. Révész, "A joint study of the Kolmogorov-Smirnov and the Eicker-Jaeschke statistics," *Statist. Decisions*, vol. 1, pp. 57–65, 1982.
[34] F. W. Scholz and M. A. Stephens, "K-sample Anderson-Darling tests," *J. Amer. Stat. Assoc.*, vol. 82, no. 399, pp. 918–924, Sep. 1987.
[35] R. Bamler and P. Harti, "Synthetic aperture radar interferometry," *Inverse Probl.*, vol. 14, no. 4, pp. R1–R54, Aug. 1998.
[36] F. De Zan and F. Rocca, "Coherent processing of long series of SAR images," in *Proc. IGARSS*, Seoul, Korea, 2005, pp. 1987–1990.
[37] A. M. Guarnieri and S. Tebaldini, "On the exploitation of targets statistics for SAR interferometry applications," *IEEE Trans. Geosci. Remote Sens.*, vol. 46, no. 11, pp. 3436–3443, Nov. 2008.
[38] P. Shanker and H. Zebker, "Persistent scatterer selection using maximum likelihood estimation," *Geophys. Res. Lett.*, vol. 34, no. 22, p. L22301, Nov. 2007.
[39] A. Hooper and H. Zebker, "Phase unwrapping in three dimensions with application to InSAR time series," *J. Opt. Soc. Amer. A, Opt. Image Sci.*, vol. 24, no. 9, pp. 2737–2747, Sep. 2007.
[40] A. M. Guarnieri and S. Tebaldini, "Hybrid Cramér-Rao bounds for crustal displacement field estimators in SAR interferometry," *IEEE Signal Process. Lett.*, vol. 14, no. 12, pp. 1012–1015, Dec. 2007.

**Alessandro Ferretti** (M'03) was born in Milan, Italy, in 1968. He received the B.S. degree (*cum laude*) in electronic engineering at the Politecnico di Milano (POLIMI) Technical University, Milano and the M.Sc. degree in information technology from CEFRIEL, Milano, working on digital signal processing, in 1993 and the D.Sc. degree in electrical engineering from the POLIMI, Milano, in July 1997.

In May 1994, he joined the radar group of the Politecnico working alongside professors Fabio Rocca and Claudio Prati on satellite radar interferometry and digital elevation model reconstruction. After devoting most of his research efforts on multi-temporal SAR data stacks at the Department of Electronics, he developed together with Prof. Rocca and Prof. Prati what is now called the "Permanent Scatterer Technique," a technology patented in 1999 that can overcome most of the difficulties encountered in conventional SAR interferometry. In March 2000, he founded, together with Prof. Rocca, Prof. Prati, and POLIMI the company "Tele-Rilevamento Europa" (TRE), first POLIMI spin-off, where he is currently the CEO. His research interest include radar data processing, optimization algorithms, data fusion, and use of remote sensing information for Civil Protection applications. Since January 2008, he is Chairman of the Board of TRE Canada Inc.

**Alfio Fumagalli** was born in Bergamo, Italy, in 1977. He received the B.S. and M.Sc. degrees in telecommunication engineering from POLIMI, Milano, Italy, in October 2002, working on Digital elevation model (DEM) generation using differential SAR interferometry.

In 2003, he joined TRE where he worked on algorithms, software development, and data integration in GIS environment. His research interests concern nonlinear systems inversion involved in PS Technique and phase unwrapping algorithms. He has been involved in many different projects related to ground surface movements detection and monitoring.

**Fabrizio Novali** was born in Bergamo, Italy, in 1975. He received the B.S. and M.Sc. degrees (*cum laude*) in telecommunication engineering at POLIMI, Milano, Italy, in April 2000, working on atmospheric effects estimation and removal in differential SAR interferometry.

In 2001, he joined TRE where he developed algorithms and associated software. His research interests include the assessment and estimation of atmospheric distortions and the detection of nonlinear motion within SAR interferogram, using the PSInSAR approach. He is project team leader of many international projects related to ground surface movements detection and monitoring. In 2004, he was appointed the Research and Development Manager of TRE.

**Claudio Prati** was born in Milano, Italy, on March 20, 1958. He is a Full Professor of Telecommunications at the Electronic Department of the POLIMI, Milano, Italy. He presently chairs the Telecommunications Study Council at POLIMI. He holds five patents in the field of SAR and SAS data processing. He published more than 100 papers on SAR data processing and interferometry. He is also co-founder of Tele-Rilevamento Europa (TRE), a RS spin-off company of POLIMI.

Mr. Prati has been awarded with two prizes from the IEEE Geoscience and Remote Sensing Society (IGARSS'89 and IGARSS'99).

**Fabio Rocca** (Specialized Graduate in Electronic Engineering, 1962) is Professor of Digital Signal Processing at POLIMI, Milano, Italy. He researched in digital signal processing for television bandwidth compression, emission tomography, seismic data processing, and SAR. From 1978 to 1988, he was a Visiting Professor at Stanford University, where he became the Department Chair from 1975 to 1978 and Commissione d'Ateneo from 1980 to 1993. He was also a cofounder of two small technological companies, Telerilevamento Europa and Aresys, a spin-off of POLIMI. He was the Past President of the EAEG, an Honorary Member of SEG (1989) and EAGE (1998), and President of OGS Trieste from 1982 to 1983. He was the Coordinator of the first EEC research program in Geosciences and a member of the Scientific Council of IN-OGS and of the SAR Advisory Group of ESA.

Mr. Rocca received the following awards: HUSPI (1979), Schlumberger (1990), Italgas for Telecommunications (1995), Special SEG Commendation (1998), Eduard Rhein Foundation for Technology (1999), Doctor Honoris Causa in Geophysics, Institut Polytechnique de Lorraine (2001). He was an Associate Editor of *Journal of Seismic Exploration* and a member of the Editorial Committee of the *Oil & Gas Science and Technology.*

**Alessio Rucci** was born in Milano, Italy, in 1982. He received the M.Sc. (*cum laude*) and D.Sc. degrees in electronic engineering from the POLIMI, Milano, in 2007 and 2011, respectively. His thesis is on advanced PInSAR technique and its application in reservoir monitoring and modeling.

In 2008, he was with Lawrence Berkeley National Lab as a Visiting Scholar to work on the InSalah Project for Carbon Capture Sequestration (CCS). In 2011, he joined the R&D division of TRE, working on the assessment and estimation of atmospheric effects and surface deformation in non-urban areas.